

Complex Nucleic Acid Hybridization Reactions inside Capillary-Driven Microfluidic Chips

Marie L. Salva, Marco Rocca, Yong Hu, Emmanuel Delamarche,* and Christof M. Niemeyer*

Nucleic acid hybridization reactions play an important role in many (bio)chemical fields, for example, for the development of portable point-of-care diagnostics, and often such applications require nucleic acid-based reaction systems that ideally run without enzymes under isothermal conditions. The use of novel capillary-driven microfluidic chips to perform two isothermal nucleic acid hybridization reactions, the simple opening of molecular beacon structures and the complex reaction cascade of a clamped-hybridization chain reaction (C-HCR), is reported here. For this purpose, reagents are arranged in a self-coalescence module (SCM) of a passive silicon microfluidic chip using inkjet spotting. The SCM occupies a footprint of $\approx 7 \text{ mm}^2$ of a $\approx 0.4 \times 2 \text{ cm}^2$ microfluidic chip. By means of fluorophore-labeled DNA probes, the hybridization reactions can be analyzed in just $\approx 2 \text{ min}$ and using only $\approx 3 \mu\text{L}$ of the sample. Furthermore, the SCM chip offers a variety of reagent delivery options, allowing, for example, the influence of the initiator concentration on the kinetics of C-HCR to be investigated systematically with minimal sample and time requirements. These results suggest that self-powered microfluidic chips equipped with a SCM provide a powerful platform for performing and investigating complex reaction systems.

involved assays.^[3] Commonly, target amplification is either performed using a thermocycling method, such as polymerase chain reaction (PCR) or ligase chain reaction (LCR), or else, employing an isothermal method, such as recombinase polymerase amplification (RPA) or rolling circle amplification (RCA).^[2a,3] Although these amplification methods have already been implemented into the microfluidic chip technologies,^[4] the involvement of enzymes can often lead to problems of reagent instability when using the chip device, thereby limiting the applicability of such chip assays for applications in POCD.^[2a,3,4a] Therefore, sensitive and selective isothermal amplification methods working at room temperature and being free of enzyme, offer a great potential in microfluidic chip-based POCDs.^[5]

The well-established hybridization-based molecular beacons (MB) reaction,^[6] the “hybridization chain reaction” (HCR)^[7]

or the recently developed “clamped-hybridization chain reaction” (C-HCR)^[8] fulfill these requirements. These reactions have the advantage of running thermodynamically stable at room temperature without the need for an enzyme and they can be monitored in real-time by fluorescence signal detection. MB reactions and HCR have already been implemented in a wide range of applications, such as in vitro multiplexed nucleic acid detection in homogeneous solutions, surface-based biosensing, or even the monitoring of enzymatic processes and living systems.^[6,7] C-HCR has so far only been used on a preparative scale for the development of macromolecular assemblies, and the initiator concentrations used are typically in the hundred micromolar range.^[8,9] The influence of the initiator concentration on the kinetics of C-HCR has not been reported so far. Furthermore, none of the previous work has included HCRs in capillary controlled microfluidic chips.

Here, we present for the first time the integration of a MB reaction and a C-HCR in capillary-driven silicon microfluidic chips, which can be examined using fluorescence signal detection. For this purpose, we use a specific structure of a microfluidic chip, called self-coalescence module (SCM), recently developed by Gökçe et al.^[10] to control the integration and homogeneous reconstitution of inkjet-spotted reagents in microfluidic chips without adverse accumulation or dispersion. A SCM enables solution-based reactions to be implemented in a controlled and precise manner inside a microfluidic chip without the need for physical compartmentalization of neighboring reactions.^[10,11] Taking advantage of the SCM,

1. Introduction

Detection of nucleic acids is of fundamental relevance for a variety of biomedical applications, such as point-of-care diagnostics (POCD).^[1] Usually, tests for nucleic acids require a signal amplification strategy to enable the detection of very low amounts of target molecules.^[2] While numerous endeavors have been made to enhance the detection and quantification of the readout signal in such diagnostic tests, there is still a need for improvement of sensitivity, specificity, and robustness of the

M. L. Salva, M. Rocca, Dr. Y. Hu, Prof. C. M. Niemeyer
Karlsruhe Institute of Technology (KIT)
Institute for Biological Interfaces (IBG-1)
Hermann-von-Helmholtz-Platz 1, Eggenstein-Leopoldshafen 76344
Germany
E-mail: niemeyer@kit.edu

M. L. Salva, M. Rocca, Dr. E. Delamarche
IBM Research Europe
Säumerstrasse 4, Ruschlikon 8803, Switzerland
E-mail: emd@zurich.ibm.com

 The ORCID identification number(s) for the author(s) of this article can be found under <https://doi.org/10.1002/sml.202005476>.

© 2020 The Authors. Small published by Wiley-VCH GmbH. This is an open access article under the terms of the Creative Commons Attribution-NonCommercial License, which permits use, distribution and reproduction in any medium, provided the original work is properly cited and is not used for commercial purposes.

DOI: 10.1002/sml.202005476

we demonstrate that a MB reaction and a C-HCR can be performed and monitored in real-time in a microfluidic chip using only a few femtomoles of spotted reagents and a few microliters of pipetted sample. The impact of the concentration of the nucleic acid target molecule that initiates both the MB reaction and C-HCR was specifically analyzed. Furthermore, we demonstrate the formation of polymeric C-HCR products, which can readily be detected, inside the capillary-driven microfluidic chip.

2. Results and Discussion

2.1. Implementation of Nucleic Acid Hybridization Reactions inside Microfluidic Chips

A SCM allows a very precise integration and handling of multiple reagents into a microfluidic chip. Hence, to investigate the implementation of complex nucleic acid hybridization reactions in capillary-driven microfluidic chips, we designed a SCM for integrating the reagents needed for the MB or C-HCR processes (Figure 1). Figure 1a illustrates the geometric features of the capillary-driven microfluidic chip, which contains a loading pad, an approximately 100-nL-volume SCM (13 mm × 530 μm × 15 μm), and an air vent to allow air displaced by the liquid to exit the chip. The figure also shows a fabricated microfluidic chip that is ≈0.4 cm × 2 cm in area and where a reference scale was patterned next to the SCM to help spotting reagents where intended and to provide a simple visual reference during experiments. As detailed in Figure S1, Supporting Information, 72 chips were fabricated on a single 4-inch silicon wafer. Briefly, two standard photolithography

steps were used to define sequentially a 8-μm-high capillary pinning line (rail patterned in the middle of the SCM) and 15-μm-high microchannels (sidewalls of the SCM and other microchannels forming the flow path).

Using an inkjet printer, reagents (≈38 nL) were spotted on one side of the capillary pinning line and allowed to dry in a few seconds. The microfluidic chip with the exception of the loading pad was then sealed by the lamination of a dry film resist. When a sample is pipetted by hand to the loading pad, it is drawn into the SCM by capillary forces. The image in Figure 1b illustrates how an incoming liquid initially fills the area of the SCM where no reagents are present by following the capillary pinning line, which acts as a Laplace pressure barrier. Once the liquid reaches the end of the SCM, it then flows over the capillary pinning line with a transient flow that wets and reconstitutes the reagents with negligible dispersion (Figure 1c).^[10] This fast and local reconstitution of reagents, without significant accumulation or Taylor–Aris dispersion, allows well-defined reactions to be carried out in pre-defined areas of the SCM. The distance between deposited spots of reagents can be tuned so as to avoid diffusion of reagents from an area to another one, if desired. Time-lapse images showing filling of a SCM are presented in Figure S2, Supporting Information.

2.2. Implementation of a MB Reaction within a SCM

Taking advantage of the possibility to define reactions in small volumes and specific areas of a SCM, we then wanted to investigate to what extent a MB reaction and a C-HCR can be implemented in a capillary-driven microfluidic chip. A MB reaction provides a self-reporting probe method that is widely employed

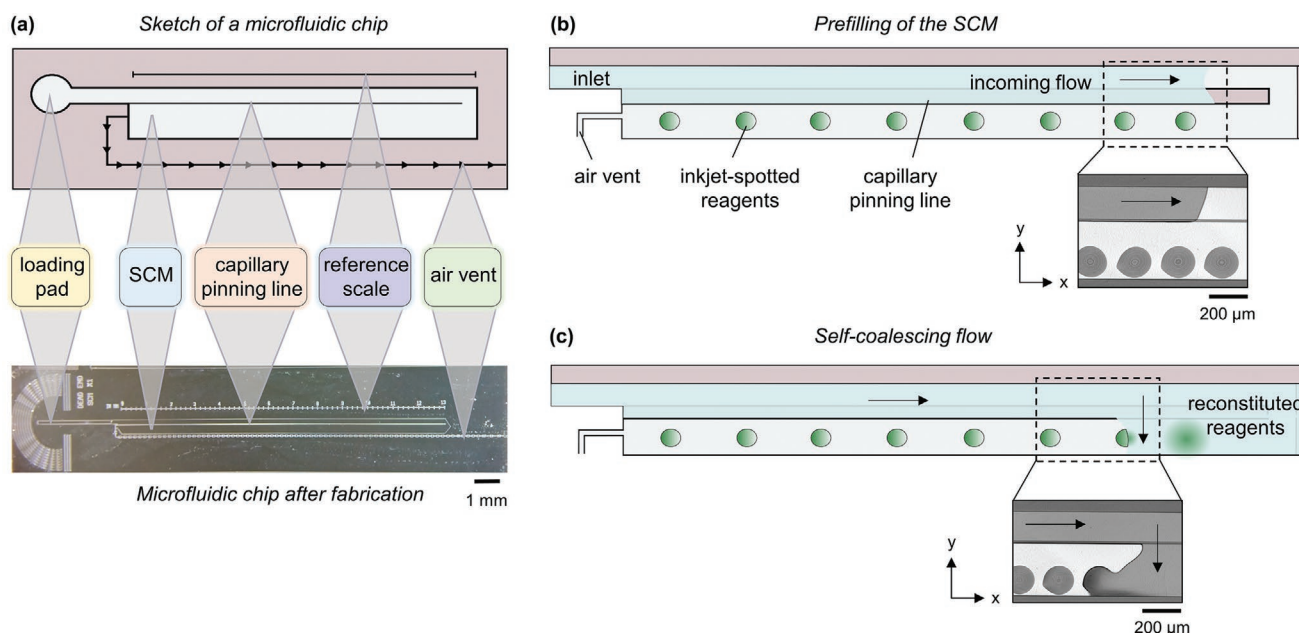


Figure 1. Implementation and working principle of a capillary-driven microfluidic chip having a SCM. a) Functional design of the microfluidic chip and photograph of a corresponding chip fabricated on a silicon wafer with photopatterned SU-8 structures. b,c) Illustration of the working principle of a SCM. The optical microscopy images (insets) show a zone of a SCM where (b) a liquid fills only the fraction of the SCM that is free of reagents by following a capillary pinning line, and (c) the self-coalescence flow during which the meniscus of liquid collapses toward the reagents, thereby wetting and reconstituting them locally.

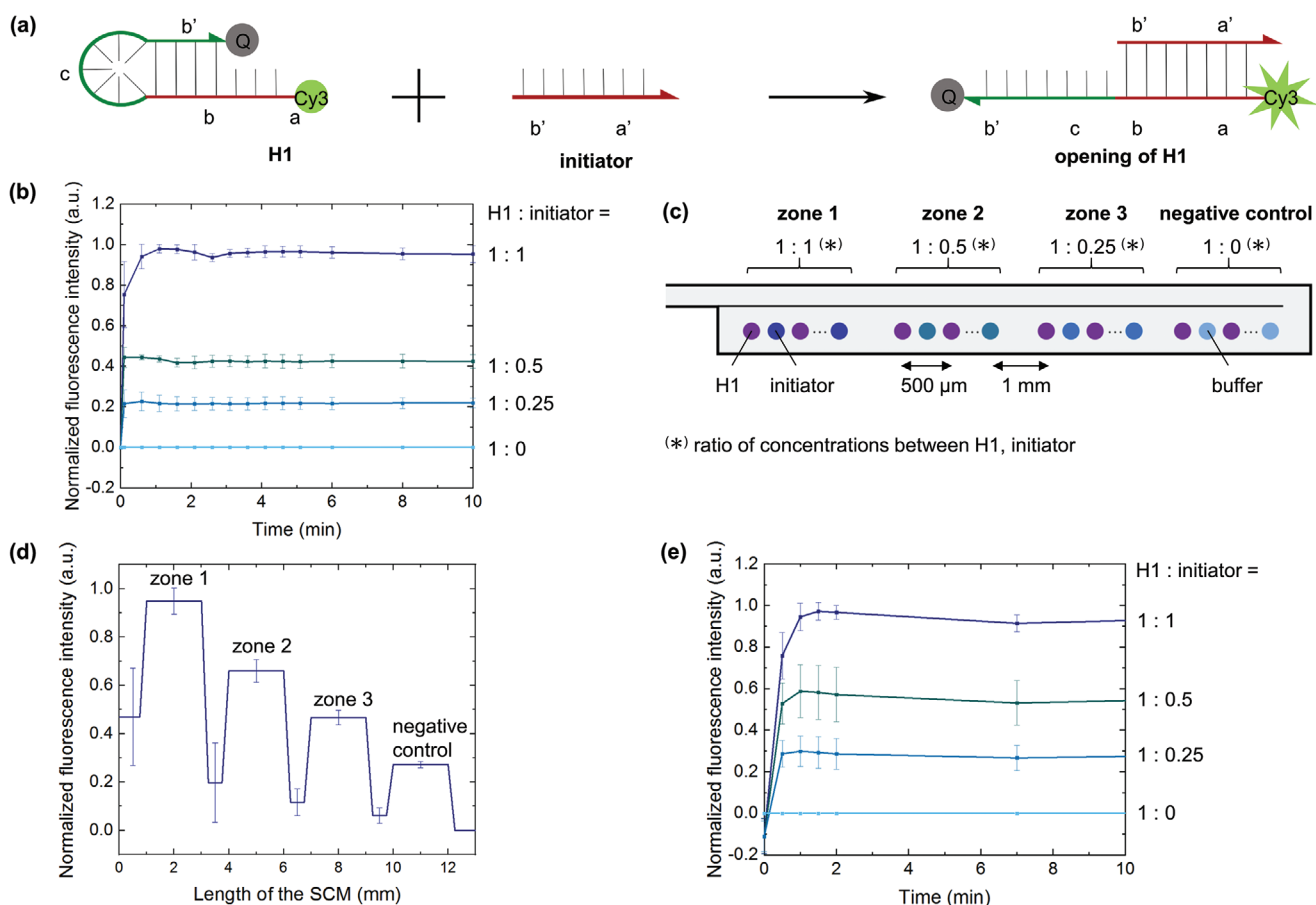


Figure 2. Implementation of a MB reaction inside a SCM and using capillary-driven flow. a) Illustration of the MB reaction. Hairpin (H1) contains a quencher (Q) and a Cy3 fluorophore tethered to one end of the oligonucleotide. Hybridization of the single-stranded initiator with the a-b regions of H1 separates Q and Cy3 thereby leading to the recovery of Cy3 fluorescence signal. b) Evolution of the normalized Cy3 fluorescence intensity over time, determined in a microtiter plate for different molar ratios of H1 and initiator. c) Sketch of the spotting pattern of the MB reagents inside the SCM. H1 and initiator was deposited in alternating order in distinctive zones of the SCM at variable molar ratios (1:1, 1:0.5, 1:0.25, and 1:0 in zones 1–4, respectively). d) Normalized fluorescence intensities determined along the main axis of the SCM at $t = 7$ min. e) Graph of the evolution of the normalized fluorescence intensity over time, measured in each zone of the SCM. The error bars in (b, d, e) represent the standard deviation obtained from 3 and 5 individual experiments, respectively. Raw data of the experiments are shown in Figure S3, Supporting Information.

in solution-based assays featuring high sensitivity and selectivity for detecting nucleic acids.^[6,12] As our work concerns the exploration of the basic possibilities of the new SCM platform, we chose an established system of oligonucleotide sequences with which both the molecular beacon reaction and the C-HCR can be performed. This has the additional advantage that the specificity of the hybridization of the oligonucleotides involved has already been verified in previous work.^[9a] We designed a MB reaction (Figure 2a) by modifying a 48-mer hairpin H1 (a/a': 6 bases, b/b': 18 bases, c: 6 bases) with a quencher (Q) at the 3' end and a fluorophore (Cy3) at the 5' end. H1 is mixed with a 24-mer single-stranded DNA (initiator). The initiator hybridizes with the a-b region of H1, to open the loop of H1 and thus separates Q from Cy3 to recover the fluorescence of the Cy3 moiety.

The formation of the molecular system depicted in Figure 2a was initially conducted in microtiter plates and verified using gel electrophoresis (Figures S3a and S3b, Supporting Information) using different ratios of H1 and initiator (1:0, 1:0.01, 1:0.02, 1:0.04, 1:0.1, 1:0.25, 1:0.5, and 1:1, respectively), whereas the

concentration of H1 was held constant. As anticipated, we observed an increased Cy3 fluorescence signal of the bands with increasing initiator concentration, thus indicating a greater amount of opened H1. As expected, the maximum fluorescence signal intensity was obtained at a molar ratio of 1:1 (Figure 2b). As expected, an excess of initiator (ratio 1:1.5) does not lead to higher fluorescence signal intensity, since all H1 molecules are opened at already equimolar amounts of the initiator (ratio 1:1, see Figure S3c, Supporting Information). We then investigated how this MB reaction takes place in a capillary-driven microfluidic chip (Figure 2c) and took advantage of localized reactions in a SCM to conduct multiple reactions in parallel. For this purpose, MB reagents were inkjet-spotted to create reaction zones covering four different concentration ratios. Each zone was 2 mm long, which represents a liquid volume of only ≈ 16 nL per zone. Zones were 1 mm apart from each other to avoid diffusion of reagents from one area to another. In each zone, the inkjet printer was used to deposit four spots of H1 alternating with four spots of initiator. Each spot was composed of 12 drops of ≈ 100 pL and the entire spotting process for creating these four zones in

the SCM was completed within ≈ 3 min. The pitch between the centers of two spots of H1 and the center of two spots of initiator was 500 μm , and therefore the distance between the center of one spot of H1 and one spot of initiator was 250 μm . The concentration of the spotted reagents was set to yield a 6 μM concentration of reconstituted H1 in each zone and a concentration of 6, 3, 1.5, or 0 μM for the initiator present in zones 1–4.

After lamination of the microfluidic chip, ≈ 3 μL of buffer was pipetted into the loading pad of the chip and the SCM autonomously filled within 45 s. The evolution of the fluorescence signal along the main axis (i.e., length) of the SCM was recorded using a fluorescence microscope for at least 7 min. The resulting spatially resolved distribution of the fluorescence signals in the SCM is shown in Figure 2d. Each curve represents the normalized average value of the fluorescence signal from five independent experiments measured in each zone of the SCM. For reasons of clarity, only one error bar per zone is shown. It can be clearly seen that the fluorescence intensity varies significantly in the different zones of the SCM as a result of having different amounts of initiator. The increased fluorescence in the negative control is due to non-quenched Cy3 fluorescence, which is stronger in the microscopic analysis of the chip than in the microtiter plate reader experiment. It can also be seen that the fluorescence signal between the different zones of the SCM rises steadily as the concentration of initiator increases, which can be explained by the lateral diffusion of DNA.

The temporal development of the fluorescence signals in the SCM chip is shown in Figure 2e. The fluorescence signal saturates in less than 2 min and remains stable for a prolonged time. To allow for a comparison between the MB reactions in the SCM and the microplate, the fluorescence data were normalized to the negative control (ratio H1:initiator = 1:0). Interestingly, the delay in measuring the reaction in a microtiter plate imposed by the pipetting and mixing steps, makes the reaction much harder to follow initially than when it is performed in the SCM. The trend for the signal evolution for varying amounts of initiator is otherwise similar for MB reactions in a microtiter plate (Figure 2b) or miniaturized in a SCM (Figure 2e). This clearly shows that solution-based nucleic acid reactions can be reproduced in a SCM and using capillary-driven flow.

2.3. Implementation of a C-HCR within a SCM

The C-HCR is a variation of the HCR,^[7] which has recently been developed to enable the site-selective deposition of self-assembled DNA polymer materials onto solid substrates^[8] and solid-liquid interfaces.^[9a] Similarly as described above for the MB reaction, we designed a C-HCR system with a quencher Q and a fluorophore Cy3 to monitor and visualize the formation of DNA polymers in SCMs (Figure 3a). The system contains the 52-mer hairpin H2 and the dimer H3-H3'. The latter was assembled from a double-labeled oligonucleotide H3' containing the quencher Q and the Cy3 dye tethered to the 3' and 5' end, respectively, and an unlabeled version of the same oligonucleotide.

After annealing, H2 can form a hairpin while H3 and H3' strands form a hairpin-dimer through the palindromic hybridization. H2 and H3-H3' coexist metastably in the absence of

an initiator since long stems (b/b': 18 bases in H2 and H3-H3') avoid short loops (a: 10 bases in H2 and c: 6 bases in H3-H3') to hybridize with toeholds (c' in H2 and a in H3-H3'). Figure S4, Supporting Information, shows a detailed schematic illustration of this C-HCR process. Once the initiator is added to the mixture of H2 and H3-H3', it first binds to the toehold region of H3-H3' and opens the long stem and short loop through DNA strand displacement reaction. Next, the active H3-H3' opens and activates an H2 through the same mechanism. Then, the latter opens another H3-H3', which repeats this reaction sequence. Importantly, since one H3-H3' has two branches, it can form (with one initiator and one H2) a three-arm junction or a four-arm junction (with two H2) to enable downstream divergent chain reactions. These processes lead to the separation of Q from Cy3 and thus the formation of a fluorescent DNA polymer.

In preliminary tests, the production and composition of the H3-H3' dimer were first optimized to avoid fluorescence self-quenching in the resulting polymer. For this purpose, different mixing ratios of unlabeled H3 and double-labeled H3' hairpins were tested. These tests showed that a proportion of 16.7% of double-labeled hairpin H3' yielded the best results (Figures S5 and S6, Supporting Information). Hence, this ratio was used for all following experiments. The C-HCR reagents (H2, H3-H3' dimer, initiator) were then inkjet-spotted into the SCM, similarly as described above for the MB reaction (Figure 3b). Again, we focused on investigating the influence of the initiator concentration on the intensity of the fluorescence signal by examining four different concentration ratios between H2, H3-H3' and initiator (1:1:0, 1:1:0.04, 1:1:0.1 and 1:1:0.25, respectively). To this end, four different zones in the SCM were as well inkjet spotted with C-HCR reagents. In each zone, four spots of a solution containing the same concentration of H2 and H3-H3' and four spots of solutions of variable initiator concentrations were alternately deposited by inkjet spotting (Figure 3b). The concentration of spotted reagent solution was set to yield a concentration of 6 μM of H2, H3-H3' in all zones after reconstitution of the reagents with buffer and a concentration of 1.5, 0.6, 0.24, and 0 μM of the initiator in zones 1-4, respectively.

After lamination of the microfluidic chip, 3 μL of buffer was pipetted into the loading pad and generation of fluorescence signals in each zone of the SCM was analyzed by fluorescence microscopy. For control purposes, reactions were performed under identical concentration conditions in a conventional microtiter plate format. The resulting spatially resolved distribution of the fluorescence signals in the SCM is shown in Figure 3c. The curve represents the normalized average value of the fluorescence signal from eight independent experiments measured in each zone of the SCM. For reasons of clarity, only one error bar per zone is shown. It can be seen that the fluorescence intensity varies in the different zones of the SCM due to different amounts of the initiator. It is also evident from Figure 3c that the level of baseline fluorescence in between the different zones does not increase steadily with increasing initiator concentration, as it is the case for the MB reaction (Figure 2d). This difference could be indicative of a lower diffusion-based mass transport between the compartments and possibly caused by the polymeric C-HCR reaction products, which might restrict diffusion between the different

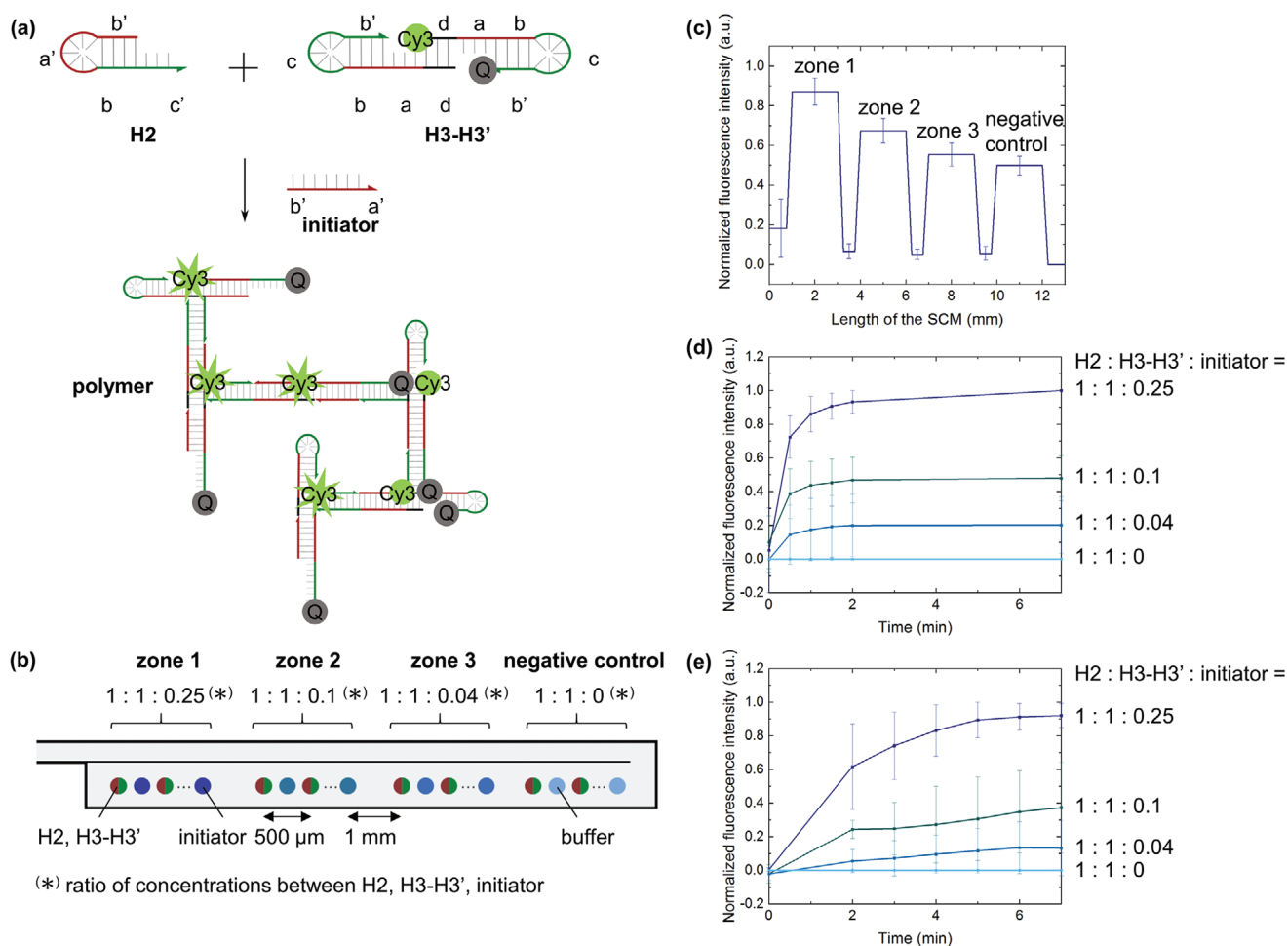


Figure 3. Implementation of a C-HCR inside a SCM and capillary-driven microfluidic chip. a) Illustration of the C-HCR. The hairpin H2 and the dimer H3-H3' containing quencher Q and a Cy3 fluorophore hybridize in the presence of the single-stranded initiator to form a fluorescent polymer (for details, see text and Figure S4, Supporting Information). b) Sketch of the spotting pattern of the C-HCR reagents inside the SCM. An equimolar amount of H2 and H3-H3' and variable amounts of the initiator were deposited in alternating order in distinctive zones of the SCM (1:1:0.25, 1:1:0.1, 1:1:0.04, and 1:1:0 in zones 1–4, respectively). c) Normalized fluorescence intensities determined along the main axis of the SCM at t = 7 min. d) Graph of the evolution of the normalized fluorescence intensity over time, measured in each zone of the SCM. e) Evolution of the normalized fluorescence intensity over time, measured for the same reactions in a microtiter plate format. The error bars in all graphs represent the standard deviations obtained from at least 3 independent experiments. Raw data of the experiments are shown in Figure S7, Supporting Information.

zones. The time-dependent generation of the fluorescence signals is shown in Figures 3d,e. The results indicate that the C-HCR was as fast as the MB reaction described above. Likewise, higher concentrations of initiator lead to the higher fluorescence signal intensity, as expected. This applies to both series of experiments performed either in the microplate or in the SCM. However, a direct comparison of time-dependent signal evolution indicates that the C-HCR occurs faster in the SCM than in the microplate. We attribute the faster reaction rate in the microfluidic chip to an initially higher concentration of reagents that are spotted in the SCM. Furthermore, we could clearly identify the formation of ≈ 5 to $7 \mu\text{m}$ thick fluorescent polymer materials in the SCM chips (Figure S7e, Supporting Information). These results nicely illustrate that a complex nucleic acid hybridization reaction like C-HCR can be readily implemented within a SCM of a capillary-driven microfluidic chip.

3. Conclusion

Nucleic acid detection is of great interest in biomedical applications, in particular, for biosensing and performing in vitro diagnostics. In this work, we demonstrated for the first time that complex nucleic acid reactions can be implemented inside capillary-driven microfluidic chips by taking advantage of self-coalescing flows and their manifestations in a SCM for realizing local, well-defined reactions. The fabrication of microfluidic chips having SCMs is simple and only involves two photolithography masks and standard photolithography steps. Fluorescence signal amplification can be completed in the chips within ≈ 2 min for both the MB reaction and C-HCR. This feature can be particularly interesting for the implementation of solution-based POCD applications that require both high detection sensitivity and short signal development times. However, it was not our intention to develop a prototype diagnostic test on

the new SCM platform, but rather to explore the basic capabilities of this device to perform complex nucleic acid hybridization reactions. The SCM chip used in this work offers a variety of options for reagent delivery. We have used this opportunity to demonstrate that the SCM chip makes it possible to investigate the influence of initiator concentration on the kinetics of C-HCR systematically and with low sample and time consumption. Such studies have not been performed so far.

Based on these results, we believe that our work is of fundamental importance for developing novel technological tools that enable the investigation of complex supramolecular reactions, such as DNA-based materials, which are currently attracting great interest.^[13] The combination of C-HCR with an SCM seems particularly powerful for performing complex reactions in self-powered microfluidics. The system we have described allows the rapid investigation of different reaction conditions in very small volumes on a very small device footprint.

In addition to their usefulness for the advancement of basic sciences, our results could open the door to a wide range of applications in the field of biomedicine and POCD. While detection of nucleic acid analytes with hand-held devices is already state-of-the-art,^[5] more complex reaction formats are required for high-sensitivity detection of proteins through nucleic acid-amplified immunoassays,^[14] such as immuno-PCR^[15] or proximity ligation assays.^[16] Therefore, the system presented here could be used not only for the detection of pathogens using nucleic acids, but also for serological tests, for example, to determine the immunity and exposure of hosts to different pathogens.

4. Experimental Section

Material, Chemicals, and Biological Chemicals: Oligonucleotides were purchased from Sigma-Aldrich and were adapted from a previous report^[8] (Table 1). The quencher at the 3' end of the sequences was an Onyx Quencher (OQ) B. Tris for buffer solutions, EDTA disodium salt 2-hydrate (Reag. Ph. Eur.) for analysis, ACS were purchased from PanReac AppliChem, ITW Reagents, Germany. Tetramethylethylenediamine (TEMED), ammonium persulfate (APS) 10%, and acrylamide 30% for gel preparations were purchased from Sigma-Aldrich. Water was distilled using the Q-Gard 2, Milli-Q (Merck). Magnesium acetate tetrahydrate (98% crystalline), DNA loading dye (6X orange DNA), DNA ladder (O'RangeRuler 50 bp, 0.05 $\mu\text{g}\cdot\mu\text{L}^{-1}$ ready-to-use), 96-well non-treated black microtiter plates, and isopropanol were purchased from Thermo Fisher Scientific. Acetone was purchased from Merck, Tween-20 Reagent from VWR international US, GelRed for gel staining from Biotium, and

dry film resists (DF-1050) from EMS Inc. US. Plate films for microtiter plates (LLG-PCR-Plattenverschlüsse QPCR) were purchased from Häberle lab, Germany. 1X TAE-Mg²⁺ was prepared in distilled H₂O (40 mM Tris, 20 mM acetic acid, 2 mM EDTA, 12.5 mM magnesium acetate, pH = 8.0). Tris buffers for the separating gel (1.5 M Tris, pH = 8.8) and for the stacking gel (1 M Tris, pH = 6.8) were prepared in distilled H₂O. Albumin-fraction V (pH = 7.0, PanReac AppliChem, ITW Reagents, Germany) was used to prepared BSA into distilled TAE-Mg²⁺. The green food dye was purchased from V2 FOODS. All preparations were made and used at room temperature.

Annealing Procedure for Forming Hairpin Structures: Lyophilized DNA was re-suspended in 1X TAE-Mg²⁺ (H1 for the MB reaction and H2, H3, and H3' for the C-HCR). H3-H3' was specifically prepared by mixing H3-H3 and H3'-H3' into different concentration ratios (3:1, 5:1, 10:1, and 20:1), as explained in Figure S5, Supporting Information. The re-suspended DNA solution was heated at 95 °C for 5 min, and then quickly quenched by cooling in ice for 2 min. The resulting solution was kept at room temperature for the rest of the preparation of the experimental samples.

Experiments in Microtiter Plate: Experiments were performed in a 96-well black microtiter plate. The total volume of liquid in each well was fixed at 50 μL . For the MB reaction, the concentration of H1 was fixed at 6 μM in each well and solutions of initiators at different concentrations (0, 0.06, 0.12, 0.24, 0.6, 1.5, 3, 6, and 9 μM) were pipetted into the corresponding wells just before starting the measurement. For the C-HCR, each well contained a solution of equal concentration of H2 and H3-H3' (6 μM). Different concentrations of initiator (0, 0.12, 0.24, 0.6, and 1.5 μM) were pipetted into the corresponding wells just before starting the measurement. The microtiter plate was then sealed with a plate film to avoid evaporation during the acquisition. Measurements were taken using a Synergy H1 Hybrid Multi-Mode Microplate Reader (BioTek Instruments, US), a Xenon Flash light source with an excitation wavelength of 540 nm, an emission wavelength of 568 nm, and a gain of 80. Graphs were plotted with the software OriginLab (Origin, Version 2018, OriginLab Corporation, MA, US).

Gel Electrophoresis: Gel electrophoresis analyses were performed using 6% w/v native polyacrylamide gel electrophoresis (Native PAGE). A 6% separating gel was first prepared by mixing in the following order (amount of reagents given for 4 gels) 10.6 mL of H₂O, 4 mL of acrylamide 30%, 5 mL of Tris buffer (pH = 8.8), 0.2 mL of APS and 0.016 mL of TEMED (APS and TEMED were added at the end) into a 50 mL Eppendorf tube. The mixture was poured into the gap between two electrophoresis glass slides (from Bio-Rad) until ≈ 2 cm below the short plate end. Ethanol was added on top of the poured gel to fill the remaining space between the plates. The gel polymerized in ≈ 1 h, the ethanol was removed and the rest of it evaporated during the preparation of the stacking gel. Then, a 5% stacking gel was prepared by mixing 5.5 mL of H₂O, 1.3 mL of acrylamide 30%, 1.0 mL of Tris buffer (pH = 6.8), 0.08 mL of APS, and 0.008 mL of TEMED into a 50 mL Eppendorf tube (amount of reagents given for 4 gels). The mixture was poured into the remaining gap between the glass slides and a 10 pockets comb was inserted between the plates. The polymerization of the gel took ≈ 1 h and the gels were then stored into a wet paper at 4 °C. 20 μL of samples prepared from 3.33 μL loading dye, 8.67 μL 1X TAE-Mg²⁺, and samples from the kinetic experiment were loaded onto the pockets of the gel. The gels were typically run at a voltage of 120 V for ≈ 50 min in 1X TAE-Mg²⁺ running buffer and subsequently stained with GelRed (5 μL into 50 mL of TAE-Mg²⁺) under orbital shaking for ≈ 1 h, according to manufacturer's instructions. Photographs were taken using a chemiluminescence gel imaging system ProteinSimple, FluorChemM Imaging system (Biozym, Germany). Pre-staining photographs were taken with a green light, orange filter, 5 s exposure time, and post-staining photographs with a blue light, green filter, and 1 s exposure time.

Microfluidic Chips Fabrication: Microfluidic chips were designed using the software L-Edit from Mentor Graphics and fabricated on a 4-inch Si wafer. A 8- μm high and 10- μm wide capillary pinning line was patterned in SU-8 (SU-8 3010 MicroChem Corp., Massachusetts USA) following a standard lithography process. The walls of the microfluidic channel were

Table 1. DNA sequences.

| Name | 5' Mod | Sequence (5'-3') | 3' Mod |
|-----------|--------|--|--------|
| Initiator | — | CTA GAG CAC AAT CAC AGG AGC CAG | — |
| H1 | Cy3 | CT GGC TCC TGT GAT TGT GCT CTA GAC ATC GCT AGA GCA CAA TCA CAG G | Q |
| H2 | — | CTA GAG CAC AAT CAC AGG AGC CAG TTT TCC TGT GAT TGT GCT CTA GCG ATG T | — |
| H3 | — | GAT CGC GAT CCT GGC TCC TGT GAT TGT GCT CTA GAC ATC GCT AGA GCA CAA TCA CAG G | — |
| H3' | Cy3 | GAT CGC GAT CCT GGC TCC TGT GAT TGT GCT CTA GAC ATC GCT AGA GCA CAA TCA CAG G | Q |

≈15-μm high and were also patterned in SU-8. The surface of the wafer was protected for dicing using an AZ4562 photoresist. The microfluidic chips were diced to create 8 stripes having multiple chips to facilitate lamination afterward. The chips were stored in black plastic wafer boxes until the spotting of reagents. Physical parameters of the microfluidic chip and specific contact angle measurements to show the feasibility of the chip are given in Figure S8, Supporting Information.

Reagents Integration in a SCM of a Microfluidic Chip: Microfluidic chips were cleaned in acetone and isopropanol and quickly dried using a stream of N₂. Pictures of the chips were taken using a smartphone camera. Five solutions (four of DNA reagents and one of buffer) were inkjet-spotted into the SCM using a Nanoplotter 2.1 inkjet spotter, a piezoelectric pipetting tip Pico – Tip J A070-402 p01116A (GeSiM, Dresden) and the software NPC16 with a spotting protocol prepared using the software SpotFrontEnd version 1.6 (GeSiM, Dresden). A total volume of 30 μL of DNA spotting solution was prepared for each reagent to be spotted (H1, initiators, and a mixture of H2, H3-H3'). For that, re-suspended DNA reagents were mixed with TAE-Mg²⁺ containing 0.002% v/v Tween-20 and BSA (0.2%) to avoid unspecific bindings of the reagents on the microfluidic surfaces and on the dry film resist. The concentrations of the 30 μL DNA solutions were calculated in order to have a specific concentration of reagents in each zone of the SCM after reconstitution of the reagents. For the negative control zone, a buffer (TAE-Mg²⁺ containing 0.002% v/v Tween-20 and BSA 0.2%) was spotted. Details of the spotted and desired concentrations after reconstitution of the reagents are given in Tables S1 and S2, Supporting Information, for the MB reaction and for the C-HCR, respectively. Each spotting solution was then pipetted into a microtiter plate inside the Nanoplotter for spotting. Spotting of the different solutions was carried out at 0.5 mm from the silicon surface at a deposition rate of ≈125 Hz. The piezoelectric tip actuated with a voltage 40–70 V (usually 60 V) and a pulse width of ≈32 μs. Each spot was formed of 12 drops (total volume of ≈1200 pL). The four zones of the SCM contained alternately four spots of H1 (resp. mixture of H2, H3-H3' for the C-HCR) and four spots of initiator. The distance between the centers of two spots of the same reagent in a zone was 500 μm. The distance inter-spots in a zone was 250 μm and the distance between two zones was 1 mm. Chips were sealed after spotting by lamination using a dry film DF-1050 resist and a hot plate (RCT basic, Staufen, IKA, Germany) with a temperature set to 45 °C.

Experiments in Microfluidic Chips: 3 μL of buffer (TAE-Mg²⁺ containing 0.002% v/v Tween-20 and BSA 0.2%) was pipetted into the loading pad of a microfluidic chip attached on a microscope glass slide. The glass slide was quickly inverted and placed on the microscope stage. Bright-field images of Figure 1 were taken with a microscope Axiovert 200M (Zeiss, Germany) using a camera AxioCam MRm (Zeiss, Germany), a 5× objective, a LED light source (Zeiss HXP 120 C lighting unit, Germany) set on 2.4 V intensity and 14ms exposure time. For Figure S2, Supporting Information, a green food dye prepared into the same buffer as reported previously was spotted into a SCM. Each drop was composed of 12 drops and separated by 250 μm. The images were taken using a self-made Lego-microscope equipped with an 8-megapixel CMOS camera and a moving stage both controlled by a Raspberry Pi Zero W (github.com/IBM/Microscopy). Fluorescence images were taken under a microscope Axio Observer Z1/7 (Zeiss, Oberkochen, Germany) using a camera Prime – 95B (Photometrics, Tucson, AZ, USA), a 10× objective, a Cy3 filter, a 50% intensity LED light source (LED-Module 555 nm), a 548 nm excitation wavelength, a 561 nm emission wavelength and a 100 ms exposure time. Time-lapse images were performed under fluorescence by taking 1 picture every 30s during the first 2 min of the acquisition and every 5 min for the next 10 min (resp. 5 min) for the MB experiment (resp. C-HCR). Image processing was performed using the software Fiji. The intensity of the fluorescence signal was evaluated using the mean gray value over each zone (2 mm × 530 μm for zones with reagents and 1 mm × 530 μm for zones without) of the SCM. Curves were plotted using the software OriginLab. Optical confocal images of DNA polymers were taken using an LSM 880 AxioObserver microscope from Zeiss, a 20× objective, a laser light

source with a gain at 700, a 561 nm excitation wavelength, a 579 nm emission wavelength, and an Airyscan detector. 3D reconstruction was performed using Ayriscan processing. The contact angles measurements of Figure S8, Supporting Information, were measured using the self-made Lego-microscope.

Supporting Information

Supporting Information is available from the Wiley Online Library or from the author.

Acknowledgements

The authors thank Y. Temiz from IBM and A.-K. Schneider from KIT for discussions and H. Riel (IBM) and T. Scharnweber (KIT) for their continuous support. This work received funding from the European Union's Horizon 2020 research and innovation program under the grant agreement no. 764476.

Open access funding enabled and organized by Projekt DEAL.

Conflict of Interest

The authors declare no conflict of interest.

Keywords

capillary-driven chip, clamped-hybridization chain reaction, molecular beacon reaction, self-coalescence module, signal amplification

Received: September 3, 2020

Revised: October 22, 2020

Published online: November 17, 2020

- [1] a) P. Yager, G. J. Domingo, J. Gerdes, *Annu. Rev. Biomed. Eng.* **2008**, *10*, 107; b) F. B. Myers, L. P. Lee, *Lab Chip* **2008**, *8*, 2015; c) A. Niemi, T. M. Ferguson, D. S. Boyle, *Trends Biotechnol.* **2011**, *29*, 240; d) L. Zhang, B. Ding, Q. Chen, Q. Feng, L. Lin, J. Sun, *TrAC, Trends Anal. Chem.* **2017**, *94*, 106; e) J. L. Cantera, H. White, M. H. Diaz, S. G. Beall, J. M. Winchell, L. Lillis, M. Kalnoky, J. Gallarda, D. S. Boyle, *PLoS One* **2019**, *14*, e0215756.
- [2] a) J. Ikbali, G. S. Lim, Z. Gao, *TrAC, Trends Anal. Chem.* **2015**, *64*, 86; b) P. Craw, W. Balachandran, *Lab Chip* **2012**, *12*, 2469.
- [3] N. Liu, F. Huang, X. Lou, F. Xia, *Sci. China: Chem.* **2017**, *60*, 311.
- [4] a) C. D. Ahrberg, A. Manz, B. G. Chung, *Lab Chip* **2016**, *16*, 3866; b) S. Lutz, P. Weber, M. Focke, B. Faltin, J. Hoffmann, C. Müller, D. Mark, G. Roth, P. Munday, N. Armes, O. Piepenburg, R. Zengerle, F. Von Stetten, *Lab Chip* **2010**, *10*, 887; c) C. Phipattanaphiphop, K. Leksakul, R. Phatthanakun, A. Suthummapiwat, *Micromachines* **2019**, *10*, 647.
- [5] M. Mauk, J. Song, H. H. Bau, R. Gross, F. D. Bushman, R. G. Collman, C. Liu, *Lab Chip* **2017**, *17*, 382.
- [6] K. Wang, Z. Tang, C. J. Yang, Y. Kim, X. Fang, W. Li, Y. Wu, C. D. Medley, Z. Cao, J. Li, P. Colon, H. Lin, W. Tan, *Angew. Chem., Int. Ed.* **2009**, *48*, 856.
- [7] S. Bi, S. Yue, S. Zhang, *Chem. Soc. Rev.* **2017**, *46*, 4281.
- [8] J. Wang, J. Chao, H. Liu, S. Su, L. Wang, W. Huang, I. Willner, C. Fan, *Angew. Chem., Int. Ed.* **2017**, *56*, 2171.

- [9] a) Y. Hu, M. Grosche, S. Sheshachala, C. Oelschlaeger, N. Willenbacher, K. S. Rabe, C. M. Niemeyer, *Angew. Chem., Int. Ed.* **2019**, *58*, 17269; b) D. Ye, M. Li, T. Zhai, P. Song, L. Song, H. Wang, X. Mao, F. Wang, X. Zhang, Z. Ge, J. Shi, L. Wang, C. Fan, Q. Li, X. Zuo, *Nat. Protoc.* **2020**, *15*, 2163.
- [10] O. Gökçe, S. Castonguay, Y. Temiz, T. Gervais, E. Delamarche, *Nature* **2019**, *574*, 228.
- [11] E. Hemmig, Y. Temiz, O. Gökçe, R. D. Lovchik, E. Delamarche, *Anal. Chem.* **2020**, *92*, 940.
- [12] S. Tyagi, F. R. Kramer, *Nat. Biotechnol.* **1996**, *14*, 303.
- [13] Y. Hu, C. M. Niemeyer, *Adv. Mater.* **2019**, *31*, 1806294.
- [14] M. Spengler, M. Adler, C. M. Niemeyer, *Analyst* **2015**, *140*, 6175.
- [15] a) T. Sano, C. L. Smith, C. R. Cantor, *Science* **1992**, *258*, 120; b) M. Adler, R. Wacker, C. M. Niemeyer, *Analyst* **2008**, *133*, 702.
- [16] a) M. Gullberg, S. Fredriksson, M. Taussig, J. Jarvius, S. Gustafsdottir, U. Landegren, *Curr. Opin. Biotechnol.* **2003**, *14*, 82; b) B. Koos, G. Cane, K. Grannas, L. Löf, L. Arngården, J. Heldin, C. M. Clausson, A. Klaesson, M. K. Hirvonen, F. M. S. De Oliveira, V. O. Talibov, N. T. Pham, M. Auer, U. H. Danielson, J. Haybaeck, M. Kamali-Moghaddam, O. Söderberg, *Nat. Commun.* **2015**, *6*, 7294.